

REPORT DOCUMENTATION PAGE

Form Approved
OMB NO. 0704-0188

Public Reporting burden for this collection of information is estimated to average 1 hour per response, including the time for reviewing instructions, searching existing data sources, gathering and maintaining the data needed, and completing and reviewing the collection of information. Send comment regarding this burden estimates or any other aspect of this collection of information, including suggestions for reducing this burden, to Washington Headquarters Services, Directorate for information Operations and Reports, 1215 Jefferson Davis Highway, Suite 1204, Arlington, VA 22202-4302, and to the Office of Management and Budget, Paperwork Reduction Project (0704-0188,) Washington, DC 20503.

| | | | | | |
|---|--|---|--|--|--|
| 1. AGENCY USE ONLY (Leave Blank) | | 2. REPORT DATE | | 3. REPORT TYPE AND DATES COVERED | |
| 4. TITLE AND SUBTITLE | | | | 5. FUNDING NUMBERS | |
| 6. AUTHOR(S) | | | | | |
| 7. PERFORMING ORGANIZATION NAME(S) AND ADDRESS(ES) | | | | 8. PERFORMING ORGANIZATION REPORT NUMBER | |
| 9. SPONSORING / MONITORING AGENCY NAME(S) AND ADDRESS(ES) U. S. Army Research Office P.O. Box 12211 Research Triangle Park, NC 27709-2211 | | | | 10. SPONSORING / MONITORING AGENCY REPORT NUMBER | |
| 11. SUPPLEMENTARY NOTES The views, opinions and/or findings contained in this report are those of the author(s) and should not be construed as an official Department of the Army position, policy or decision, unless so designated by other documentation. | | | | | |
| 12 a. DISTRIBUTION / AVAILABILITY STATEMENT Approved for public release; distribution unlimited. | | | | 12 b. DISTRIBUTION CODE | |
| 13. ABSTRACT (Maximum 200 words) | | | | | |
| 14. SUBJECT TERMS | | | | 15. NUMBER OF PAGES | |
| | | | | 16. PRICE CODE | |
| 17. SECURITY CLASSIFICATION OR REPORT UNCLASSIFIED | | 18. SECURITY CLASSIFICATION ON THIS PAGE UNCLASSIFIED | | 19. SECURITY CLASSIFICATION OF ABSTRACT UNCLASSIFIED | |
| | | | | 20. LIMITATION OF ABSTRACT UL | |

NSN 7540-01-280-5500

Standard Form 298 (Rev.2-89)
Prescribed by ANSI Std. 239-18
298-102

Enclosure 1

Research Article

Stable Transmission in the Time-Varying MIMO Broadcast Channel

Adam L. Anderson,¹ James R. Zeidler,¹ and Michael A. Jensen²

¹Department of Electrical and Computer Engineering, University of California, San Diego, CA 92093-0407, La Jolla, USA

²Department of Electrical and Computer Engineering, Brigham Young University, Provo, UT 84602, USA

Correspondence should be addressed to Adam L. Anderson, a3anders@ucsd.edu

Received 1 June 2007; Revised 28 September 2007; Accepted 19 December 2007

Recommended by Christoph Mecklenbräuer

Both linear and nonlinear transmit precoding strategies based on accurate channel state information (CSI) can significantly increase available throughput in a multiuser wireless system. With propagation delay, infrequent channel updates, lag due to network layer overhead, and time-varying node position or environment characteristics, channel knowledge becomes outdated and CSI-based transmission schemes can experience severe performance degradation. This paper studies the performance of precoding techniques for the multiuser broadcast channel with outdated CSI at the transmitter. Traditional channel models as well as channel realizations measured by a wideband channel sounder are used in the analysis. With measured data from an outdoor urban environment, it is further shown the existence of stable subspaces upon which transmission is possible without any instantaneous CSI at the transmitter. Such transmissions allow for consistent performance curves at the cost of initial suboptimality compared to CSI-based schemes.

Copyright © 2008 Adam L. Anderson et al. This is an open access article distributed under the Creative Commons Attribution License, which permits unrestricted use, distribution, and reproduction in any medium, provided the original work is properly cited.

1. INTRODUCTION

The time-varying, multiuser, multiple-input multiple-output (MIMO) wireless channel promises significant gain in performance over that offered by conventional single-antenna systems [1]. Multiplexing and multiple access gains increase system throughput and are achieved through the use of multiple antennas and spatial reuse. Temporal diversity gains enabled by channel-time variation further increase system performance. Unfortunately, this temporal variation typically implies that outdated estimates of the channel state information (CSI) are used to construct the signaling strategy, resulting in capacity degradation [2, 3] that is analogous to that created by channel estimation errors [4, 5]. These same effects of channel estimation errors and Doppler sensitivity in practical precoding systems were shown in [6, 7] to contribute significantly to performance loss. These observations motivate the development of transmission schemes which are robust to physically-realistic channel variations.

Prior work has studied performance degradations of the single-user, point-to-point MIMO link when transmitter

and receiver have channel estimation errors or partial CSI. In [4] capacity upper and lower bounds are given for the single-user, flat-fading, MIMO channel with Gaussian inputs and normal channel error statistics. The work in [3] uses measured channel responses for moving nodes to analyze the capacity degradation caused by outdated CSI at the transmitter (CSIT) and receiver (CSIR). In an effort to reduce this sensitivity to CSI quality, recent research has suggested the formation of transmit beamformers using channel distribution information (CDI) at the transmitter (CDIT) [8, 9], a strategy which is optimal in an ergodic capacity sense under certain antenna correlation conditions. An adaptive beamformer that uses both CSI and CDI is suggested in [10] where capacity degradation from outdated CSI occurs in a time division duplex (TDD) MIMO system with a spatially correlated Jakes' channel.

Similar work for the multiuser MIMO channel has focused more on the effects of channel estimation errors than the impact of outdated CSI created by channel-time variation. For example, for the single-input single-output (SISO) broadcast channel, a scheduling strategy was proposed in [11] to combat the effects of channel estimation error.

Furthermore, capacity regions for the MIMO broadcast channel with erroneous CSIT and CSIR are found in [12] using the duality between the broadcast and multiple-access channels (MAC) [13]. The work in [5] uses error statistics for the sum-capacity-optimal dirty-paper coding (DPC)[1] to determine when time-sharing outperforms DPC in the multiple-input single-output (MISO) broadcast channel. A similar study for erroneous CSIT was also performed for the computationally simpler zero-forcing DPC (ZF-DPC) in [14] using capacity bounds similar to those presented in [4].

This work builds on the existing understanding to study the behavior of different CSIT-based transmit precoding techniques [15] in the time-variant multiuser broadcast channel (BC). The study considers DPC, linear beamforming, and time-division multiple access (TDMA) techniques. While numerous beamforming algorithms exist for various design criteria [15–17] we focus on the beamforming algorithm that maximizes capacity for a MIMO broadcast channel (for linear precoding) as defined in [15] which is an extension of the algorithm in [18] for (MISO) channels. The TDMA scheme removes multiple access interference (MAI) and the need for CSIT by assigning each user a unique time slot for channel access and by using the optimal signaling strategy for an uninformed transmitter. The analysis of these schemes begins with simulations based on accepted models for the spatially-correlated time-variant channel [19, 20]. However, since these models may not capture the complex physical structure of the multiuser time-variant MIMO channel [21], the results obtained using the models are reinforced using simulations with experimentally obtained channels [22] taken in an outdoor environment on the Brigham Young University (BYU) campus [3, 23]. Motivated by the performance degradation observed for the existing signaling schemes, the paper finally develops and analyzes an iterative beamforming algorithm that has similar performance to the capacity optimal beamformer when used with CSIT and provides stable throughput performance when constructed with CDIT. The stable performance offered by this algorithm implies the existence of slowly varying subspaces in the time-varying multiuser MIMO channel.

2. SYSTEM AND CHANNEL MODELS

The MIMO broadcast channel communication scenario of interest consists of a single transmitting node equipped with N_t antennas and K receiving nodes (users) each with N_r antennas. The $N_r \times 1$ received vector for the j th user at time sample n can be expressed as

$$\mathbf{y}_j(n) = \mathbf{H}_j(n)\mathbf{x}_j(n) + \sum_{i \neq j}^K \mathbf{H}_j(n)\mathbf{x}_i(n) + \boldsymbol{\eta}_j(n), \quad (1)$$

where $\mathbf{H}_j(n)$ is the $N_r \times N_t$ matrix of channel transfer functions for user j , $\mathbf{x}_i(n)$ is the $N_t \times 1$ signal vector destined for the i th user, and $\boldsymbol{\eta}_j(n)$ is additive white Gaussian noise (AWGN). Equation (1) presumes no specific transmit precoding and is therefore appropriately modified later in the discussion of specific transmission schemes.

The examination of different precoding strategies performed in this paper considers both modeled channels, which allow a parametric evaluation over a variety of channel conditions but may not accurately represent the physical time-space evolution of the subspace, and measured channels which allow performance quantification over a limited set of realistic environments. This section details the models and measurements used to facilitate this study.

2.1. Channel models

Because effective multi-antenna transmit precoding strategies exploit spatial structure in the channel, it is important that the channel model used accurately reflects this spatial information. The spatial correlation of the transfer matrix, which is created by the angular properties of the multipath propagation as well as the antenna configuration, is a common mechanism for capturing this spatial structure in the model. To aid in the analysis, the correlation matrices at the transmit and receive ends of the link are assumed separable, resulting in a Kronecker description of the overall spatial correlation [20]. Using this mechanism, the channel matrix at the n th time sample is

$$\mathbf{H}_j(n) = \sqrt{\mathbf{R}_{r,j}}\mathbf{H}_{w,j}(n)\sqrt{\mathbf{R}_{t,j}}, \quad (2)$$

where $\mathbf{H}_{w,j}(n)$ is an $N_r \times N_t$ matrix with zero mean, unit variance, i.i.d. complex Gaussian random variables at sample index n , $\mathbf{R}_{r,j}$, and $\mathbf{R}_{t,j}$ are the $N_r \times N_r$ and $N_t \times N_t$ receive and transmit correlation matrices, respectively, for the j th user, and the square root operation on some positive semidefinite matrix \mathbf{Z} is defined as $\sqrt{\mathbf{Z}}\sqrt{\mathbf{Z}} = \mathbf{Z}$. There is some debate on the accuracy of the Kronecker model because the model has been verified for a small number of antennas in [24] while deficiencies in the model for a larger number of antennas have been identified in [25]. The application of interest in this work is a mobile ad hoc network (MANET) in which all nodes are equally equipped with a small number of antennas, justifying the use of the Kronecker model assumption in (2).

Any model must also ensure that the channel samples possess the proper relationship in time. This can be accomplished by properly representing the temporal correlation between channel samples for sample spacings smaller than the channel coherence time. This work assumes the temporal correlation function model suggested by Jakes [19] which is given by

$$\rho(\tau) = J_0(2\pi f_d \tau), \quad (3)$$

where $J_0(\cdot)$ is the zeroth-order Bessel function of the first kind and f_d is the normalized Doppler frequency. For simulation purposes a sum of eight weighted sinusoids is used in Jakes' model with the specified normalized Doppler taken into account to produce the temporal correlation in (3).

The channel model realizes both spatially and temporally correlated channel coefficients by filtering $\mathbf{H}_{w,j}(n)$ in (2) with the time-varying coefficients generated from Jakes' model with the Doppler frequency f_d in (3) chosen to match that of the measured channel. Further, the spatial correlation matrices used in (2) are either modeled with an

exponentially decaying function or estimated from measured data as explained in Section 2.2. The channel matrices for different users are realized independently. Throughout this paper, the term “modeled channel” refers to a sequence of channel matrices generated using this procedure.

2.2. Channel measurements

The test equipment at BYU allows sampling of a single-user point-to-point MIMO link with $N_r = N_t = 8$. The measurements can accommodate up to 100 MHz of instantaneous bandwidth at a center frequency between 2 and 8 GHz. Specific details of the measurement equipment are available in [26].

Prior to data collection, calibration measurements were taken with the transmitter “off” to measure background interference. At the chosen carrier frequency of 2.45 GHz, the external interference was found to be below the noise floor in the environment considered. A second calibration performed with both the transmitter and receiver “on” but stationary revealed that the time variation of the channel caused by ambient changes such as pedestrians, atmospheric conditions, and other natural disturbances was insignificant for the environments examined in this paper.

The channel coefficients used in this analysis were measured with a stationary transmitter and a receiver moving at a constant pedestrian velocity (30 cm/s). Since the channel is highly oversampled, with samples taken every 3.2 milliseconds, data decimation or interpolation can be used to create any effective node velocity. For a given transmitter location, measurements for different receiver locations were taken (using the same receiver velocity), with each location producing the channel matrix for one user in (1) for the simulated multiuser network. Since it was observed that channel-time variation results almost exclusively from node movement, the superposition of these asynchronous measurements into a single-synchronized multiuser broadcast channel seems reasonable. Throughout this paper the term “measured channel” refers to channel coefficients acquired in this fashion.

The statistical space-time-frequency structure of the experimental MIMO channels has been well analyzed in the literature [2, 27] with ensemble averages over a variety of locations showing the coefficients to obey a zero-mean complex Gaussian distribution (Rayleigh channel magnitudes) with spatial and temporal correlation functions that closely resemble those generated using the classic Jakes model [23]. Because the transmit and receive spatial correlation matrices are used in the development of the transmit precoding strategy introduced in this paper as well as the generation of modeled channel matrices (see Section 2.1), estimation of these matrices from the data is an important consideration. The transmit correlation matrix estimated using N samples starting at sample n_0 can be written as

$$\mathbf{R}_{t,j}(n_0, N) = \frac{1}{NN_r} \sum_{n=0}^{N-1} \mathbf{H}_j^H(n_0 + n) \mathbf{H}_j(n_0 + n), \quad (4)$$

where $\{\cdot\}^H$ is the matrix conjugate transpose. Similarly, the receive correlation matrix estimate is

$$\mathbf{R}_{r,j}(n_0, N) = \frac{1}{NN_t} \sum_{n=0}^{N-1} \mathbf{H}_j(n_0 + n) \mathbf{H}_j^H(n_0 + n). \quad (5)$$

The fact that the correlation matrices are functions of the starting channel index n_0 and length of the estimate N suggests that the channel is *not* stationary. This nonstationarity is a mathematical manifestation of physical changes in the propagation environment created by changes in the angular characteristics of the propagation environment due to such effects as a node moving around a corner or the introduction of a mobile scatterer. However, drastic nonstationary effects occur on a time scale larger than the channel coherence time, and therefore values of N are chosen to remain within the channel stationarity time.

3. TRANSMIT PRECODING WITH TIME-VARYING CHANNEL

Transmit precoding techniques attempt to manipulate input data signals to achieve a specified design criterion for the overall system. The types of precoders can be classified as either linear or nonlinear [15] while system optimizations range from maximizing throughput to minimizing transmit power for a given signal-to-interference plus noise (SINR) requirement. Regardless of the scheme or optimization used, most algorithms require instantaneous CSIT. This requirement suggests that as nodes move and CSIT becomes outdated, the performance guarantee of an algorithm no longer holds. This section describes the optimal sum capacity technique (DPC), linear transmit beamforming (BF), and time division multiple access (TDMA), and evaluates their performance degradation due to node motion.

It is important to choose a measurable quantity such that comparison between different algorithms can be performed in a meaningful manner. For this work, we consider performance metrics based on maximizing the total mutual information between transmitter and receiver for all users given the theoretical concept of Gaussian input signals [4]. For a given transmit precoding algorithm with fixed input parameters, the total mutual information is referred to as either the expected sum rate or throughput of the system measured in bits/sec/Hz.

To calculate the sum mutual information for the broadcast channel with outdated CSIT, a general procedure is followed for all transmit precoding techniques. First, the CSIT (assumed perfect) obtained when the receivers are at an initial position is used to generate the precoded transmit vectors over a range of receiver motion, meaning that the CSIT used is outdated except at the initial position. The received vector for each user is then determined using (1), allowing computation of the mutual information for each user, and the sum mutual information is computed as the sum of each individual mutual information value.

3.1. Optimal transmit precoding

The nonlinear dirty-paper coder is optimal in the sense that it maximizes the sum mutual information (and therefore sum capacity) when the receivers are at their initial position. Consider the case of strict DPC at the transmitter, where user 1 is encoded first, user 2 second, and so on. The iterative implementation of the algorithm results in received vectors at sample n given CSIT $\mathbf{H}_j(n_0)$ obtained at sample $n_0 \leq n$ given by

$$\mathbf{y}_j(n_0, n) = \begin{cases} \mathbf{H}_1(n)\mathbf{x}_1(n) + \mathbf{H}_1(n) \sum_{i=2}^K \mathbf{x}_i(n) + \boldsymbol{\eta}_1(n), & j = 1, \\ \mathbf{H}_j(n)\mathbf{x}_j(n) + \mathbf{E}_j(n_0, n) \sum_{i=1}^{j-1} \mathbf{x}_i(n) + \mathbf{H}_j \sum_{i=j+1}^K \mathbf{x}_i(n) + \boldsymbol{\eta}_j(n), & 2 \leq j \leq K, \end{cases} \quad (6)$$

where $\mathbf{E}_j(n_0, n) = \mathbf{H}_j(n) - \mathbf{H}_j(n_0)$.

The mutual information for the j th received vector in (6) given knowledge at the receiver of *both* $\mathbf{H}_j(n)$ and $\mathbf{H}_j(n_0)$ is

$$I_{\text{DPC}}[\mathbf{x}_j(n); \mathbf{y}_j(n_0, n) \mid \mathbf{H}_j(n), \mathbf{H}_j(n_0)] = h[\mathbf{y}_j(n_0, n) \mid \mathbf{H}_j(n)] - h[\mathbf{y}_j(n_0, n) \mid \mathbf{x}_j(n), \mathbf{H}_j(n), \mathbf{H}_j(n_0)], \quad (7)$$

where $\mathbf{x}_j(n)$ are assumed to be Gaussian inputs and $h[\cdot]$ is the entropy function. With perfect CSIR, the error becomes deterministic at the receiver (i.e., the receiver is aware that CSIT is outdated), and therefore both $[\mathbf{y}_j(n_0, n) \mid \mathbf{H}_j(n), \mathbf{H}_j(n_0)]$ and $[\mathbf{y}_j(n_0, n) \mid \mathbf{x}_j(n), \mathbf{H}_j(n), \mathbf{H}_j(n_0)]$ are Gaussian distributed. As a result, the upper and lower bounds on mutual information with erroneous CSI from [4] are equivalent and reduce to

$$I_{\text{DPC}}[\mathbf{x}_j(n); \mathbf{y}_j(n_0, n) \mid \mathbf{H}_j(n), \mathbf{H}_j(n_0)] = \log \frac{|\mathbf{Z}_j + \mathbf{H}_j(n)\mathbf{Q}_j(n_0)\mathbf{H}_j^H(n)|}{|\mathbf{Z}_j|}, \quad (8)$$

$$\mathbf{Z}_j = \mathbf{I} + \sum_{i=j+1}^K \boldsymbol{\Psi}_j^{\mathbf{H}_i(n)} + \sum_{i=1}^{j-1} \boldsymbol{\Psi}_j^{\mathbf{E}_i(n_0, n)},$$

where for some matrix \mathbf{V} , $\boldsymbol{\Psi}_j^{\mathbf{V}} = E[\mathbf{V}^H \mathbf{Q}_j(n_0) \mathbf{V}]$ and $\mathbf{Q}_j(n_0) = E[\mathbf{x}_j(n_0)\mathbf{x}_j^H(n_0)]$ represents the input covariance matrix calculated at sample n_0 . After computing (8) for each user, the sum mutual information becomes

$$C_{\text{DPC}}(n_0, n) = \sum_{j=1}^K I_{\text{DPC}}[\mathbf{x}_j(n); \mathbf{y}_j(n_0, n) \mid \mathbf{H}_j(n), \mathbf{H}_j(n_0)], \quad (9)$$

where $C_{\text{DPC}}(n_0, n)$ is implicitly a function of the input covariance matrices $\mathbf{Q}_i(n_0)$. If the transmitter assumes that there is no lag between acquisition of CSIT and transmission

(i.e., inaccurately assumes $n = n_0$), then the ‘‘optimum’’ input covariances are found using the duality of the MAC/BC and iterative water-filling [1].

3.2. Linear transmit precoding

Linear transmit precoding, or beamforming, is a technique that uses linear preprocessing to mitigate multiuser interference. Different types of BF algorithms are used to optimize different communication parameters [15]. Because we are considering techniques which maximize the sum mutual information, we adopt a rate-maximizing BF technique [18]. In this case, the $N_t \times 1$ capacity optimal beamformer weights $\mathbf{b}_j(n_0)$ for user j are computed at sample index n_0 based upon the CSIT $\mathbf{H}_j(n_0)$. Assuming a maximum of one data stream is transmitted to each user, the received signal vector for user j at sample $n \geq n_0$ is

$$\mathbf{y}_j(n_0, n) = \mathbf{H}_j(n)\mathbf{b}_j(n_0)x_j(n) + \mathbf{H}_j(n) \sum_{i \neq j}^K \mathbf{b}_i(n_0)x_i(n) + \boldsymbol{\eta}_j(n). \quad (10)$$

Because the distributions of both the desired signal and the interference plus noise given $\mathbf{H}_j(n)$ are Gaussian, the mutual information for user j is found in a manner similar to that outlined in Section 3.1, resulting in

$$I_{\text{BF}}[\mathbf{x}_j(n); \mathbf{y}_j(n_0, n) \mid \mathbf{H}_j(n), \mathbf{H}_j(n_0)] = \log \frac{|\mathbf{I} + \mathbf{H}_j(n) \left(\sum_{i=1}^K \mathbf{Q}_i(n_0) \right) \mathbf{H}_j^H(n)|}{|\mathbf{I} + \mathbf{H}_j(n) \left(\sum_{i \neq j}^K \mathbf{Q}_i(n_0) \right) \mathbf{H}_j^H(n)|}, \quad (11)$$

where $\mathbf{Q}_j(n_0) = E[\mathbf{b}_j(n_0)\mathbf{b}_j^H(n_0)]$ and $E[\mathbf{x}_j^H(n)\mathbf{x}_j(n)]$ is unity. If the optimization results in the zero matrix for $\mathbf{Q}_j(n_0)$, then user j is excluded from access to the channel. For completeness, we can write the total expected rate given the outdated input covariances $\mathbf{Q}_i(n_0)$ for beamforming as

$$C_{\text{BF}}(n_0, n) = \sum_{j=1}^K I_{\text{BF}}[\mathbf{x}_j(n); \mathbf{y}_j(n_0, n) \mid \mathbf{H}_j(n), \mathbf{H}_j(n_0)]. \quad (12)$$

Some comments are necessary regarding the capacity maximizing MISO beamforming algorithm [18]. In [15], this technique was used with multiple receive antennas by iteratively performing the algorithm while updating the receiver beamformer with minimum mean squared error (MMSE) weights, although no proof of optimality was made. Since the beamforming weights are, in form, capacity optimal (CO) for the MISO channel and have the structure of a regularized channel inversion (RCI), it is referred to here as CO-RCI [15].

3.3. Time division multiple access without CSIT

Time division multiple access (TDMA) is a transmit precoding technique that ideally creates an interference-free environment. Furthermore, since it does not require CSIT,

it can provide stable throughput in a time-varying channel although it significantly lowers the overall throughput since it does not accommodate simultaneous channel access for multiple users. This form of TDMA is achieved by employing time sharing at the transmitter and optimal coding with no CSIT assuming a Rayleigh fading channel. For this scheme, the broadcast channel reduces to a virtual single-user channel (\mathbf{x}_i is zero for $i \neq j$) where each user has a received vector

$$\mathbf{y}_j(n) = \mathbf{H}_j(n)\mathbf{x}_j(n) + \boldsymbol{\eta}_j(n). \quad (13)$$

Since each user is only accessing the channel a fraction of the time, the mutual information for user j will simply be

$$I_{\text{TDMA}}[\mathbf{x}_j(n); \mathbf{y}_j(n) | \mathbf{H}_j(n)] = \frac{1}{K} \log \left| \mathbf{I} + \frac{P}{N_t} \mathbf{H}_j(n) \mathbf{H}_j^H(n) \right|, \quad (14)$$

where P is the total available power at the transmitter and the optimal input covariance reduces to the scaled identity for all n_0 given channel coefficients which satisfy a spatially uncorrelated Gaussian distribution. The stability of TDMA without CSIT is manifest in the total sum mutual information

$$C_{\text{TDMA}}(n) = \sum_{j=1}^K I_{\text{TDMA}}[\mathbf{x}_j(n); \mathbf{y}_j(n) | \mathbf{H}_j(n)] \quad (15)$$

which is only a function of the current channel at sample n .

Performance comparisons between different transmit precoders can be made by examining how total throughput scales with the number of network nodes [15]. Consider the standard Rayleigh flat-fading channel scenario where there is no lag between CSIR and CSIT (i.e., $n = n_0$) and all nodes have perfect estimates of the channel. Figure 1 shows throughput scaling as the number of users increases for each of the transmit precoding techniques discussed. The system is fixed at $N_t = 4$ transmit antennas, $N_r = 4$ receive antennas per user, and a total power constraint of $P = \sum_i \text{tr}\{\mathbf{Q}_i(n_0)\} = 10$. While these results reveal the optimality of DPC, they also show that BF captures the majority of available throughput for larger networks and that the TDMA performance does not scale appreciably with increasing network size.

4. PERFORMANCE METRICS

Assessing the performance of the algorithms under consideration requires definition of meaningful metrics which capture the performance degradation created by outdated CSIT. Naturally, many different metrics could be defined, with the conclusions drawn ultimately depending on these definitions. However, since the goal of DPC and CO-RCI is to maximize the sum mutual information, it is logical that the performance metrics used in this work depend on this quantity. One excellent metric which describes the maximum rate at which error-free transmission is theoretically possible for a given channel type is the ergodic channel capacity [1]. However, computing this quantity requires an expectation

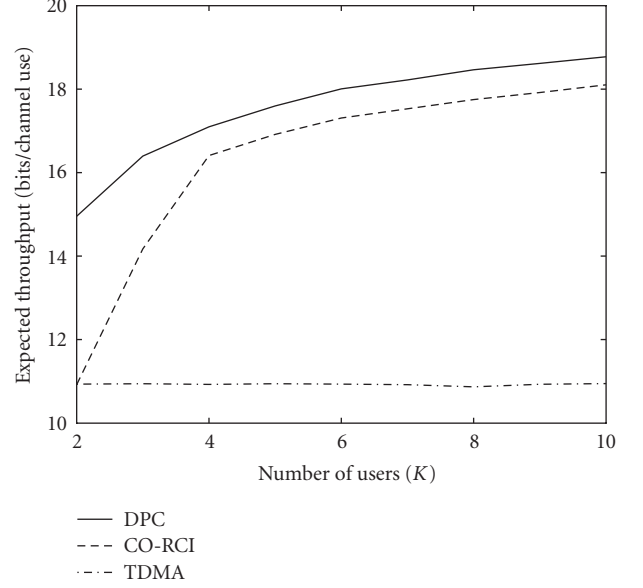


FIGURE 1: Expected throughput versus number of users for fixed $N_t = N_r = 4$ antennas and $P = 10$ in Rayleigh, flat-fading channel model. All nodes have perfect channel knowledge for all realizations of the channel.

over an infinite set of channel realizations, which is not possible using a finite set of measured data, and is not strictly defined for outdated CSI.

Given the difficulties associated with the ergodic capacity for this application, metrics used in this study are based on the sample expected throughput (SET) which is the expected error-free throughput for the channel as a function of the delay $n - n_0$. We perform a time average over all possible initial displacements n_0 , so that the SET for a displacement $\Delta_n = n - n_0$ is defined as

$$S_{\mathcal{X}}(\Delta_n) = \frac{1}{N_{\max} - \Delta_n} \sum_{m=1}^{N_{\max} - \Delta_n} C_{\mathcal{X}}(m, m + \Delta_n), \quad (16)$$

where N_{\max} is the total number of samples in the dataset and the subscript \mathcal{X} is a member of the set of specified precoders {DPC, BF, TDMA}. Note that for $\Delta_n = 0$, (16) represents the time-average expected system throughput. Since this study considers temporal channel variation and not coefficient estimation, it is assumed that the channel estimates $\mathbf{H}_j(n)$ and $\mathbf{H}_j(n_0)$ known, respectively, at the receiver and transmitter are error free.

It is noteworthy that $C_{\mathcal{X}}(n_0, n_0 + \Delta_n)$ is not necessarily a decreasing function of Δ_n . For example, if the channel estimate occurs at the end of a fade, the sum mutual information is likely to be greater as the nodes move and the channel improves. However, because the SET in (16) represents an average behavior, it generally decreases with increasing Δ_n . Figure 2 plots the SET versus the *spatial* displacement $\Delta = \Delta_n T_s v$, where T_s and v represent respectively the sample interval and the receiver velocity, for each of the transmit precoders assuming Jakes' channel model and a normalized Doppler frequency of $f_d = 0.0086$ chosen based upon T_s and

v . The system parameters include $K = 5$ users each equipped with $N_r = 4$ antennas, a transmitter with $N_t = 4$ antennas, and a total power constraint of $P = 10$. The maximum displacement Δ is limited to 3λ since the transient behavior of throughput degradation happens within this interval. Note that both DPC and CO-RCI experience a reasonably rapid degradation in throughput as a result of outdated CSIT.

While plots of the SET such as that in Figure 2 reveal detailed information regarding performance degradation due to outdated CSIT, it is useful to derive simple quantitative measures from the SET that allow single-number comparison of the behavior for different environments. The remainder of this section outlines two metrics based on the SET which help quantify the stability of the transmit precoding algorithms and motivate the new algorithm defined in Section 5.

4.1. SET crossover distance

As shown in Figure 2, there is a displacement at which the expected throughput drops below that for TDMA. This displacement, denoted as d_T , is referred to as the SET crossover distance and quantifies the displacement beyond which CSIT is no longer useful (i.e., beyond this displacement, TDMA which uses no CSIT offers higher throughput). Small values of d_T suggest that a given precoding algorithm is highly sensitive to channel temporal variations and will perform poorly in practical systems. In Figure 2, $d_T = 0$ for TDMA, $d_T \approx 0.25\lambda$ for DPC, and $d_T \approx 0.4\lambda$ for CO-RCI beamforming.

4.2. Average sample expected throughput (ASET)

While the SET crossover distance gives an indication of how quickly the performance degrades with node displacement, it clearly provides only limited insight into the behavior. This fact motivates another performance metric which incorporates the throughput over all displacements. The average sample expected throughput (ASET) is defined by

$$\bar{S}_X(M) = \frac{1}{M} \sum_{\Delta_n=0}^{M-1} S_X(\Delta_n), \quad (17)$$

where M represents the extent of displacements in the region of interest. From Figure 2, the normalized ASET values $\bar{S}_X/\bar{S}_{\text{TDMA}}$ are 1, 0.89, and 0.55 for TDMA, CO-RCI, and DPC, respectively.

Some important observations from Figure 2 can be made regarding the performance metrics and their effects on transmission stability. The distance d_T is meaningful in that it defines the sensitivity of an algorithm to node movement but is not practical as an optimizable variable. For example, maximizing d_T will not necessarily result in a stable transmission policy since the majority of available throughput may be lost in the first few fractions of a wavelength. In fact, Figure 2 indicates that the most stable transmission scheme is TDMA which maximizes the ASET. These observations will be used to motivate a more stable transmit precoder in Section 5.

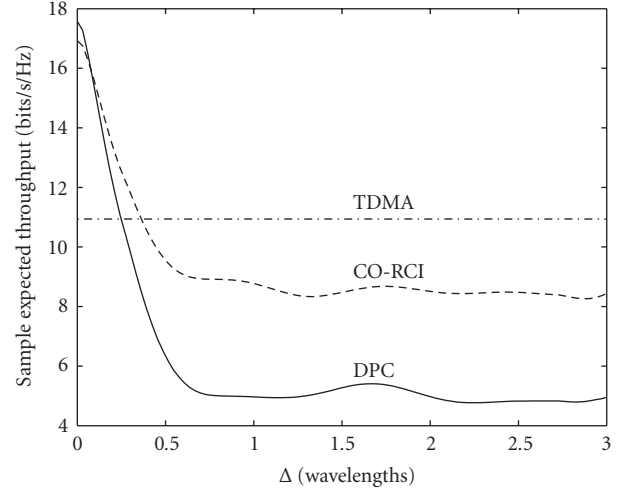


FIGURE 2: Sample expected throughput (SET) as a function of delay for a network with parameters $N_t = N_r = 4$, $K = 5$, and $P = 10$ given various transmit precoding schemes in the spatially white, Jakes' channel model with a normalized Doppler frequency of $f_d = 0.0086$.

5. STABLE TRANSMISSION

As shown in the previous sections, attempting to transmit with either the optimal nonlinear transmit precoding scheme (DPC) or linear beamforming on the optimal subspaces (CO-RCI) results in significant performance loss with even small node displacement. This observation suggests that a signaling strategy which is insensitive to node displacement must use transmission on suboptimal subspaces that remain constant for longer periods of time. Motivated by this fact, we present an iterative beamforming algorithm that has similar performance to CO-RCI beamforming when used with CSIT and stable performance when used with CDIT. While the complexity of this algorithm is higher than that of CO-RCI, it enables a significantly reduced frequency at which the transmitter BF weights must be updated.

5.1. MMSE-CSIT beamforming

Our goal is to define a beamforming algorithm that achieves the capacity-optimal performance of CO-RCI when used with CSIT but can be extended for use with CDIT. We apply the standard coordinated transmitter/receiver beamforming algorithm suggested in [15] where weights at the transmitter and receiver are updated in an iterative manner. To motivate the steps at each iteration of the algorithm, the following observations are considered:

- (i) the metric of interest is maximizing the total mutual information (capacity) of the system with linear beamforming (Section 3);
- (ii) MMSE beamforming at the receiver is capacity optimal [13];
- (iii) there exists a duality between transmit and receive beamforming [1, 13].

- (1) Assume an initial set of N_s random transmit weights \mathbf{b}_i with equal power allocation $p_i = P/N_s$
- (2) Calculate the MMSE *receiver* beamforming weights for all streams to all users

$$\mathbf{w}_{i,j} = (\mathbf{I} + \mathbf{H}_j(\sum_k p_k \mathbf{b}_k \mathbf{b}_k^H) \mathbf{H}_j^H)^{-1} \mathbf{H}_j \mathbf{b}_i p_i$$
- (3) Find the survivor streams using SINR

$$\pi(i) = \arg \max_j \rho_{i,j}$$
- (4) Numerically optimize the powers p_i assigned to each stream
- (5) Update the MMSE *transmitter* beamforming weights

$$\mathbf{b}_i = (\mathbf{I} + \sum_k p_k \mathbf{H}_{\pi(k)}^H \mathbf{w}_{k,\pi(k)} \mathbf{w}_{k,\pi(k)}^H \mathbf{H}_{\pi(k)})^{-1} \mathbf{H}_{\pi(i)} \mathbf{w}_{i,\pi(i)} p_i$$
- (6) Repeat (2)–(5) until convergence
- (7) Repeat (1)–(6) for $N_s = 1, \dots, K$
- (8) Use $\mathbf{w}_{i,\pi(i)}$ corresponding to the value of N_s that maximizes

$$C_{\text{MMSE-CSIT}} = \sum_{i=1}^{N_s} \log(1 + \rho_{i,\pi(i)})$$

ALGORITHM 1: Iterative beamforming for maximization of sample expected throughput.

For the following, the optimization variable is indexed over the current sample index n and the index n_0 at which the transmitter acquires CSI. This indexing is for convenience when we address CDI beamforming, while for CSI beamforming the transmitter assumes $n_0 = n$ for all time (i.e., the transmitter only calculates a single set of beamforming weights).

Unit norm transmit beamforming weights $\mathbf{b}_i(n_0)$ are initialized for a given number of data streams N_s using the singular vectors of a random matrix, similar to the random beamforming algorithm [28], with the powers for all streams initially equal. Given transmit weights and powers, each receiver calculates a set of N_s MMSE beamforming weights, one for each of the N_s streams. For unit receiver noise variance and assuming linear receiver processing (so that multiple streams destined for the same user will interfere with each other), the resulting received SINR of the i th stream to the j th user for the MISO broadcast channel is written as

$$\rho_{i,j}(n_0, n) = \frac{p_i(n_0) \mathbf{b}_i^H(n_0) \mathbf{H}_j^H(n) \mathbf{H}_j(n) \mathbf{b}_i(n_0)}{1 + \sum_{k \neq i} p_k(n_0) \mathbf{b}_k^H(n_0) \mathbf{H}_j^H(n) \mathbf{H}_j(n) \mathbf{b}_k(n_0)}, \quad (18)$$

where $p_i(n_0)$ is the power allocated to the i th stream and $\sum_i p_i(n_0) \leq P$.

The next step within the iteration is to assign a single user to each stream. This is accomplished by sequentially moving through each of the N_s streams and assigning to it the user which achieves the highest value of $\rho_{i,j}(n_0, n_0)$. If $\pi(i)$ represents the user index for the i th stream, this process is represented mathematically as

$$\pi(i) = \arg \max_j \rho_{i,j}(n_0, n). \quad (19)$$

It is important to note that while the stream mapping policy $\pi(i)$ may result in nodes without an assigned stream at a given iteration, these nodes may recapture a stream at a future iteration.

Once streams have been mapped to users, MMSE receiver beamforming weights are computed using

$$\mathbf{w}_{i,j}(n_0, n) = \left\{ \mathbf{I} + \mathbf{H}_j(n) \sum_{k=1}^K p_k(n_0) \mathbf{b}_k(n_0) \mathbf{b}_k^H(n_0) \mathbf{H}_j^H(n) \right\}^{-1} \times \mathbf{H}_j(n) \mathbf{b}_i(n_0) p_i(n_0). \quad (20)$$

Each receiver then “transmits” using its set of beamforming weights over the reciprocal channel $\mathbf{H}_j^H(n_0)$, and for each stream the transmitter computes updated MMSE beamforming weights $\mathbf{b}_i(n_0)$. For a given set of transmitter and receiver beamforming weights, the quasiconvexity of the single-input single-output SINR function enables a straightforward numerical optimization of the power coefficients $p_i(n_0)$ to maximize the expected system rate. The sample expected throughput based on the beamforming weights and power allocations is

$$C_{\text{MMSE-CSIT}}(n_0, n) = \sum_{i=1}^{N_s} \log(1 + \rho_{i,\pi(i)}(n_0, n)), \quad (21)$$

where (18) is modified to include both transmit and receive weights for the MIMO channel. The final solution corresponds to the weights $\mathbf{w}_{i,j}(n_0, n)$ associated with the value of N_s that maximizes (21). The complete algorithm for maximizing the sample throughput through linear processing, referred to as MMSE-CSIT, is summarized in Algorithm 1. Note that since the algorithm is performed with $n = n_0$, Algorithm 1 drops sample indices from the variable matrices.

Figure 3 compares CO-RCI and MMSE-CSIT beamforming for $N_t = 6$, $N_r = 1$, $P = 10$, and a variable number of receiver nodes for perfect CSI. The channel coefficients were generated using the standard Rayleigh, flat-fading model for the multiuser channel. Figure 3 also shows the optimal nonlinear DPC precoder as a performance reference. Note that, with power optimization, CO-RCI and MMSE-CSIT perform almost identically, which is the intended result.

When step 4 is dropped from the algorithm, equal power is used for each data stream and only a small loss in throughput is seen as the number of users increases. Figure 4 shows the convergence with the number of iterations for CO-RCI and MMSE-CSIT. Note that the trend for both algorithms is a longer convergence time as the number of users is increased. Though not shown, a similar behavior is observed as the number of antennas is increased for either the transmitter or receiver. It is noteworthy that both the CO-RCI and MMSE-CSIT algorithms only guarantee convergence to a local maximum when used in the MIMO broadcast channel, therefore allowing the situation where one algorithm outperforms the other. From a computational complexity standpoint, at each iteration the complexity of the CO-RCI algorithm is dominated by the cost of taking the inverse of a single $N_t \times N_t$ and $KN_r \times N_r$ matrices, with an asymptotic cost of $O(N_t^3 + KN_r^3)$. In contrast, the complexity of the MMSE-CSIT algorithm requires taking the inverse of approximately $KN_t \times N_t$ and $K^2N_r \times N_r$ matrices, which is roughly K times the cost of the CO-RCI scheme.

5.2. MMSE-CDIT beamforming

As observed at the end of Section 4.2 and shown in Figure 2, stable transmission is achieved by the scheme that maximizes the ASET of the channel rather than instantaneous throughput. We therefore reformulate the beamforming problem to maximize the average of (21) over some window size M , or

$$\bar{C}_{\text{MMSE-CSIT}}(n_0, M) = \frac{1}{M} \sum_{m=0}^{M-1} \sum_{i=1}^{N_s} \log(1 + \rho_{i,\pi(i)}(n_0, n_0 + m)). \quad (22)$$

While direct maximization of (22) with no CSIT appears difficult, the average throughput can be upper and lower bounded by (see the appendix for discussion on bounds)

$$\begin{aligned} \bar{C}^{\text{upper}}(n_0, M) &= \sum_{i=1}^{N_s} \log(1 + \bar{\rho}_{i,\pi(i)}(n_0, M)), \\ \bar{C}^{\text{lower}}(n_0, M) &= \sum_{i=1}^{N_s} \log(1 + \tilde{\rho}_{i,\pi(i)}(n_0, M)), \end{aligned} \quad (23)$$

where

$$\bar{\rho}_{i,\pi(i)}(n_0, M) = \frac{1}{M} \sum_{m=0}^{M-1} \frac{\text{num}\{\rho_{i,\pi(i)}(n_0, n_0 + m)\}}{\text{den}\{\rho_{i,\pi(i)}(n_0, n_0 + m)\}}, \quad (24)$$

$$\tilde{\rho}_{i,\pi(i)}(n_0, M) = \frac{(1/M) \sum_{m=0}^{M-1} \text{num}\{\rho_{i,\pi(i)}(n_0, n_0 + m)\}}{(1/M) \sum_{m=0}^{M-1} \text{den}\{\rho_{i,\pi(i)}(n_0, n_0 + m)\}}, \quad (25)$$

and $\text{num}\{\cdot\}$ and $\text{den}\{\cdot\}$ return the numerator and denominator, respectively, of the argument. Equation (24) is the average SINR (ASINR) while (25) is the ratio of the average signal power to the average interference plus noise powers (ASAINR). Analogous to the instantaneous throughput of (21), the bounds on average throughput (23) can each be

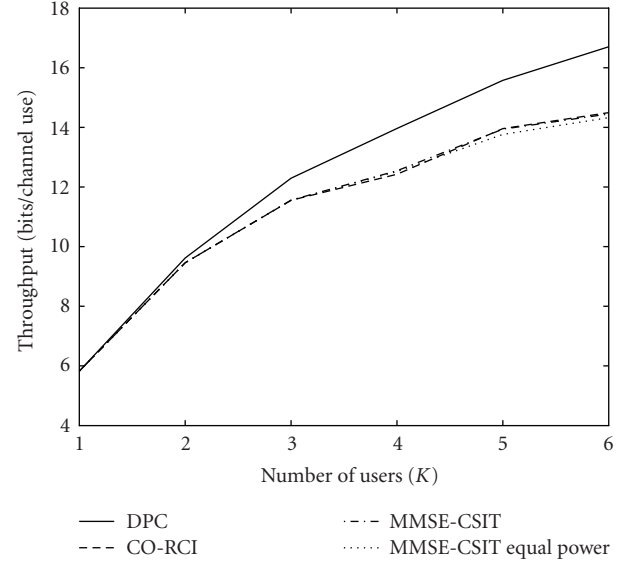


FIGURE 3: Comparison of optimal transmit beamforming CO-RCI and MMSE-CSIT beamforming for $N_t = 6$, $N_r = 1$, and $P = 10$ in a Rayleigh flat-fading channel. The optimal nonlinear preprocessing (DPC) is also shown for comparison.

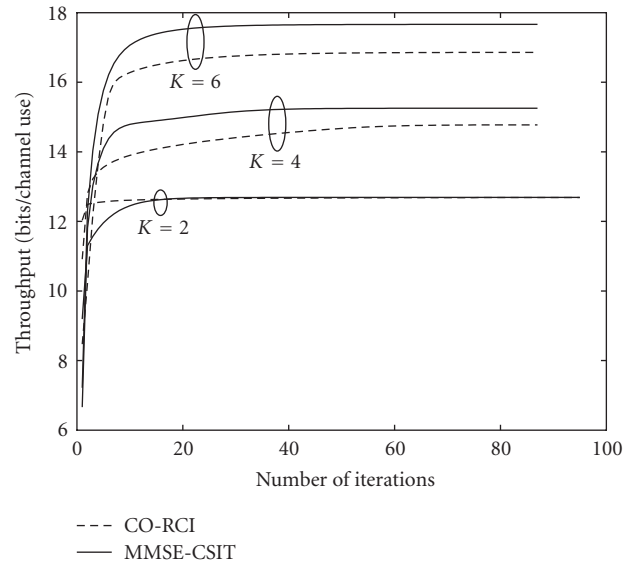


FIGURE 4: Convergence of CO-RCI and MMSE-CSIT beamforming algorithms for $N_t = 4$, $N_r = 4$, $P = 10$, and different number of users for a channel realization from the measured data.

considered instantaneous throughputs assuming the SNR is given by the average quantities ASINR and ASAINR, respectively.

Since, as shown in the appendix, the lower bound on ASET is tighter than the upper bound, we will use this bound

- (1) Assume an initial set of N_s random transmit weights \mathbf{b}_i with equal power allocation $p_i = P/N_s$
- (2) Calculate the *receiver* beamforming weights for all streams to all users

$$\mathbf{w}_{i,j} = (\mathbf{I} + \sqrt{\mathbf{R}_{t,j}}(\sum_k p_k \mathbf{b}_k \mathbf{b}_k^H) \sqrt{\mathbf{R}_{t,j}}^H)^{-1} \sqrt{\mathbf{R}_{t,j}} \mathbf{b}_i p_i$$
- (3) Find the survivor streams by using

$$\pi(i) = \arg \max_j \tilde{\rho}_{i,j}$$
- (4) Update the *transmitter* beamforming weights

$$\mathbf{b}_i = (\mathbf{I} + \sum_k p_k \sqrt{\mathbf{R}_{t,\pi(k)}}^H \mathbf{w}_{k,\pi(k)} \mathbf{w}_{k,\pi(k)}^H \sqrt{\mathbf{R}_{t,\pi(k)}})^{-1} \sqrt{\mathbf{R}_{t,\pi(i)}} \mathbf{w}_{i,\pi(i)} p_i$$
- (5) Repeat (2)–(4) until convergence
- (6) Repeat (1)–(5) for $N_s = 1, \dots, K$
- (7) Use $\mathbf{w}_{i,\pi(i)}$ corresponding to the value of N_s that maximizes

$$C_{\text{MMSE-CDIT}} = \sum_{i=1}^{N_s} \log(1 + \tilde{\rho}_{i,\pi(i)})$$

ALGORITHM 2: Iterative beamforming for maximization of ASET lower bound.

as the objective function for maximization. The ASAINR can be expanded generically as

$$\begin{aligned}
 & \tilde{\rho}_{i,j}(n_0, M) \\
 &= \frac{(1/M) \sum_{m=0}^{M-1} \text{num} \{ \rho_{i,j}(n_0, n_0 + m) \}}{(1/M) \sum_{m=0}^{M-1} \text{den} \{ \rho_{i,j}(n_0, n_0 + m) \}} \\
 &= \frac{(1/M) \sum_{m=0}^{M-1} p_i(n_0) \mathbf{b}_i^H(n_0) \mathbf{H}_j^H(a_m) \mathbf{H}_j(a_m) \mathbf{b}_i(n_0)}{1 + (1/M) \sum_{m=0}^{M-1} \sum_{k \neq i} p_k(n_0) \mathbf{b}_k^H(n_0) \mathbf{H}_j^H(a_m) \mathbf{H}_j(a_m) \mathbf{b}_k(n_0)} \\
 &= \frac{p_i(n_0) \mathbf{b}_i^H(n_0) \sqrt{\mathbf{R}_{t,j}(n_0, M)}^H \sqrt{\mathbf{R}_{t,j}(n_0, M)} \mathbf{b}_i(n_0)}{1 + \sum_{k \neq i} p_k(n_0) \mathbf{b}_k^H(n_0) \sqrt{\mathbf{R}_{t,j}(n_0, M)}^H \sqrt{\mathbf{R}_{t,j}(n_0, M)} \mathbf{b}_k(n_0)}, \quad (26)
 \end{aligned}$$

where $\mathbf{R}_{t,j}(n_0, M)$ is the transmit correlation matrix from (4) and $a_m = n_0 + m$. Note that (26) is in the exact form of (18) used for maximizing throughput with CSIT when the transmit correlation matrices are exchanged for channel realizations. Thus, the same beamforming algorithm used to maximize instantaneous throughput can also be used to maximize the lower bound on average throughput by simply swapping CDIT for CSIT. Algorithm 2 shows the beamforming algorithm that utilizes CDIT (MMSE-CDIT) with power optimization removed for computational savings.

An important discrepancy between the MMSE-CSIT and MMSE-CDIT beamformers is the use of channel duality when updating the beamformer weights. With MMSE-CSIT beamforming, the dual of the downlink channel is simply the matrix Hermitian of the uplink and vice versa. However, for MMSE-CDIT beamforming, the receive correlation matrix is *not* generally the Hermitian of the transmit correlation matrix. For example, if the transmitter is closely obstructed by interferers or contains tightly spaced antennas, then (4) will reflect more correlation than (5) and duality will not hold. For this algorithm, however, SINR equality is only required when the transmitter and receiver change roles, and this is satisfied when using $\mathbf{R}_{t,j}^H(n_0, M)$ as the dual “channel” for MMSE-CDIT.

Figure 5 plots SET for the CO-RCI and CDIT-MMSE beamformers with the TDMA scheme provided as a baseline. Channel coefficients for this plot were generated using Jakes’ model with a normalized Doppler of $f_d = 0.0086$, $N_t = N_r = 4$ antennas, $K = 5$ users, and $P = 10$. Spatial correlation is added by creating transmit correlation matrices with exponential decay where the element in the i th row and j th column is given by

$$r_{i,j} = \begin{cases} \gamma_i & i = j, \\ e^{-\alpha(i-j)^2} & i \neq j. \end{cases} \quad (27)$$

For each user, α is chosen randomly from a uniform distribution on the range $[0.5, 1]$ and γ_i is chosen to keep relative gains on par with the measured data. After adding spatial correlation to Jakes’ model, channel realizations are normalized to match the overall gain of the measured channel. Figure 5 again confirms the degradation of CO-RCI with displacement originally observed in Figure 2. However, the MMSE-CDIT beamforming provides a stable throughput and provides the maximum ASET for the algorithms considered. This result suggests that the beamforming weights produced by the MMSE-CDIT algorithm reside in stable subspaces within the multiuser time-varying MIMO channel. This stability can be seen by noting that the throughput as a function of SINR and delay is only based on the single set of beamformer weights produced at zero delay and not adapted to channel conditions and variations. It is also interesting to note that the SET crossover distance d_T for the CO-RCI beamformer in this spatially correlated channel is larger than that observed for the spatially white Jakes’ channel considered in Figure 2. This observation suggests that spatial correlation provides an innate robustness to channel temporal variation when used with linear beamforming even when the correlation is not explicitly used in the computation of the beamforming weights.

Some comments regarding the MMSE-CDIT beamforming algorithm are necessary. First, it is important to reinforce that for simulation purposes, the weights found from the iterative MMSE-CDIT algorithm are treated like standard beamforming weights of CO-RCI. In other words,

the algorithm is used to find a single set of weights, and these weights are fixed as the nodes move throughout the system. No adaptive beamforming is considered for either case. Second, one might consider using CDIT knowledge directly with either DPC or CO-RCI. However, we have observed that the resulting performance is lower than that obtained from either the MMSE-CDIT beamformer or TDMA, and therefore these approaches are not considered further in this work.

6. SIMULATION RESULTS

Full assessment of the performance of the algorithms considered in this paper requires sweeping over a large number of independent parameters, including available power at the transmitter, number of transmit and receive antennas, node velocities, channel spatial correlation, number of users, and type of scattering environment. For measured channel data, certain parameters (number of antennas, transmit power) can be altered to some degree while others (scattering environment, node velocities, number of users) are determined by the operational environment. In this section, the SET is examined for a fixed number of antennas and transmit power level. The following conditions are imposed on the simulations undertaken.

- (i) Although the ordering of users could be optimized to maximize information throughput [1], this paper is focused on the performance degradation due to channel-time variation for a specified ordering, and therefore user signal encoding is performed in a fixed order.
- (ii) The measured data can accommodate a maximum of six users in the broadcast channel.
- (iii) Prior to node movement, both transmitter and receiver share perfect (i.e., channel estimation error-free) knowledge of the channel. As nodes move, the receiver is assumed to always have the current CSI while the transmitter only has the initial channel state. This assumption suggests embedded training symbols in the transmitted signal and error-free channel estimation at the receiver with limited feedback to the transmitter.
- (iv) Only a single, outdoor environment is used for the measured data. The environment used in these simulations consists of pedestrian velocities in an urban-like area surrounded by buildings and stationary vehicles.
- (v) When spatial correlation is used with the modeled channel, the transmit correlation matrix is taken from estimates generated by the measured channel. Although results in this section are focused on the measured data, we also provide results for the modeled channel (i.e., spatially correlated Jakes' model) which allows for contrast between the two channels.

Figure 6 shows the SET of the four transmit precoders examined in this work, namely nonlinear optimal DPC,

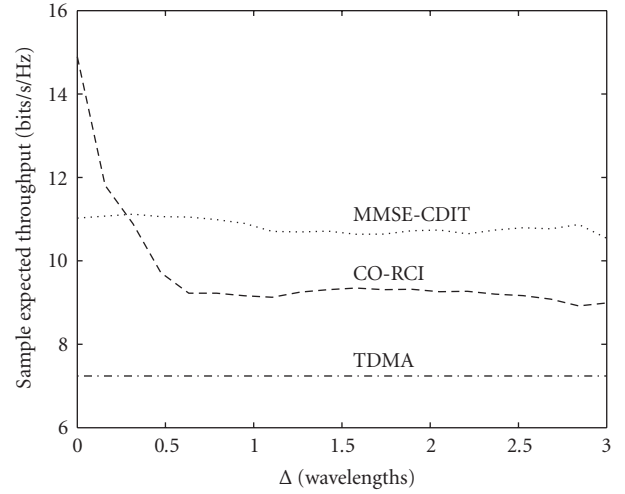


FIGURE 5: Sample expected throughput versus displacement for $N_t = N_r = 4$ antennas, $K = 5$ users, and $P = 10$ in Jakes' model with exponential spatial correlation and various transmit precoding schemes.

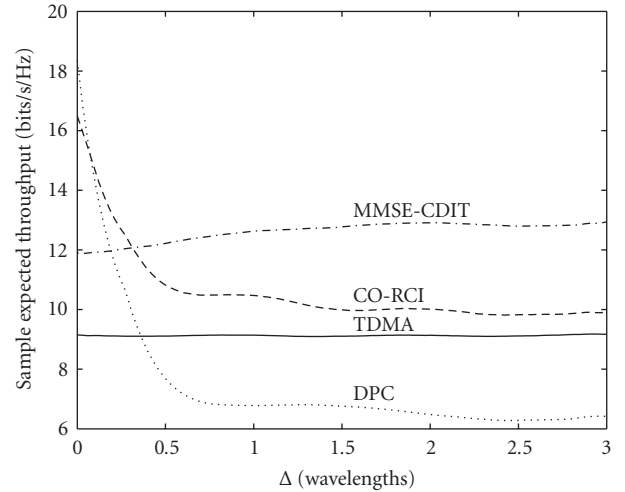


FIGURE 6: Sample expected throughput (SET) for $N_t = N_r = 4$, $K = 5$, and $P = 10$ in the measured channel with various transmit precoding schemes.

linear optimal BF (CO-RCI), the iterative beamformer presented in this paper (MMSE-CDIT), and time division multiple access (TDMA). The simulation uses the measured data with $N_t = 4$ transmit antennas and $K = 3$ users each with $N_r = 4$ antennas. The total available power is fixed at $P = 10$ and nodes are displaced at a constant pedestrian velocity. These results reveal that while DPC has the highest possible throughput, it is also the most sensitive to outdated CSIT as measured by the SET. Optimal CSIT beamforming achieves an initial performance that is near that of DPC and has a more graceful loss in performance as nodes move. MMSE-CDIT beamforming throughput performance is initially suboptimal, but remains constant throughout the length of the simulation. It is clear that

TABLE 1: Performance metrics for three transmit precoders with two channel realizations.

| | DPC | | CO-RCI | | MMSE-CDIT | |
|----------|---------------|----------------------------|--------------|-------------------------------|--------------|----------------------------------|
| Modeled | 1.43λ | 1.1 | $> 3\lambda$ | 1.327 | $> 3\lambda$ | 1.50 |
| Measured | 0.3λ | 0.79 | $> 3\lambda$ | 1.17 | $> 3\lambda$ | 1.37 |
| | d_T | $\frac{S_{DPC}}{S_{TDMA}}$ | d_T | $\frac{S_{CO-RCI}}{S_{TDMA}}$ | d_T | $\frac{S_{MMSE-CDIT}}{S_{TDMA}}$ |

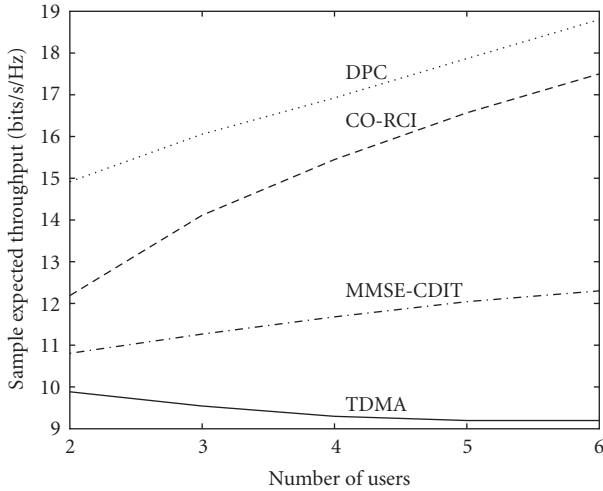


FIGURE 7: Sample expected throughput versus the number of users for $N_t = N_r = 4$ and $P = 10$ in the measured channel. There is no lag between channel acquisition and use.

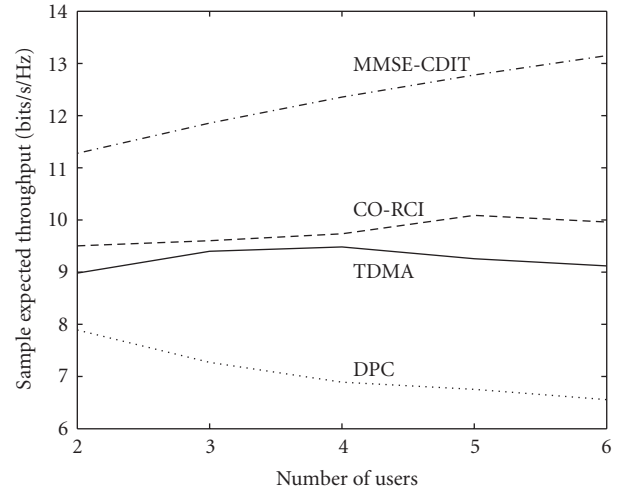


FIGURE 8: Sample expected throughput versus number of users for $N_t = N_r = 4$ and $P = 10$ in the measured channel. There is a lag of 1.5λ between channel acquisition and use.

the SET crossover distance for MMSE-CDIT is beyond the simulation region and is much larger than that of any other precoder. As a reference, the SET crossover distance (d_T) and normalized ASET (\bar{S}_X/\bar{S}_{TDMA}) for each of the transmit precoders and channel models are provided in Table 1. The differences between the results for the modeled and measured channels stem from the fact that the model does not necessarily capture the actual effects (such as temporal correlation) present in the measured channels. Despite these differences, the results for the two channel types suggest the same performance trends with the most notable one being that MMSE-CDIT beamforming outperforms all other schemes for the metrics presented. Furthermore, it appears that linear precoding even with outdated CSI provides some robustness to channel temporal variations for the given antenna correlations while the self-interference caused by nonlinear precoding significantly degrades the system.

Figure 7 demonstrates scalability of the network for different types of precoding when both transmitter and receiver are equipped with perfect channel knowledge. The simulation uses measured data with $N_t = N_r = 4$ and $P = 10$ with a variable number of receivers. These results confirm the finding from Figure 1 that all schemes that use some form of channel knowledge scale in throughput versus the number of users. Figure 8 shows the results of the same simulation performed with a displacement of

$\Delta = 1.5\lambda$ between channel update and transmission. This intriguing result reveals that the performance degradation for DPC worsens as the network size increases. MMSE-CDIT beamforming is impervious to mobility in the network within the channel stationarity time and is the only precoder that provides significant increase in performance with the number of nodes for outdated transmit channel information.

7. CONCLUSION

This paper has examined the performance loss of transmit precoding techniques in the multiuser, time-varying, MIMO broadcast channel. The performance of the optimal transmit precoding schemes was shown to be sensitive to both node movement and increasing number of users when CSIT is outdated. An iterative beamforming technique (MMSE-CDIT) was developed that uses linear preprocessing to maximize the average sample expected throughput of the system. Simulation results using both modeled and measured channels revealed that MMSE-CDIT beamforming provides high stability in terms of throughput while offering higher ASET and increased performance with the number of users when compared to TDMA. The results suggest that multiuser signaling strategies based on channel distribution information can provide good performance for multiuser mobile networks.

APPENDIX

AVERAGE SAMPLE EXPECTED THROUGHPUT (ASET) BOUNDS

Consider parameterizing the single-user, MISO, beamforming channel ergodic capacity into a function of scalar quantities as

$$C = E \left[\log \left(1 + \frac{\sigma_s^2 s}{\sigma_n^2 n} \right) \right], \quad (\text{A.1})$$

where s and n are random variables representing the signal and interference, respectively, and specific realizations are assumed known at the receiver. The quantities σ_s^2 and σ_n^2 are normalizing factors corresponding to the signal and interference powers. Equation (A.1) is the composition of a concave ($\log\{\cdot\}$) and quasiconvex (SINR) function leading to the constrained bounds

$$C^{\text{upper}} = \log \left(1 + E \left[\frac{\sigma_s^2 s}{\sigma_n^2 n} \right] \right), \quad (\text{A.2})$$

$$C^{\text{lower}} = \log \left(1 + \frac{\sigma_s^2 E[s]}{\sigma_n^2 E[n]} \right). \quad (\text{A.3})$$

Equation (A.2) is always a true upper bound from Jensen's inequality and the concavity of the logarithm. The lower bound is conditionally true since the composed ergodic capacity is a quasiconvex function [29]. A straightforward example of when the lower bound holds is when s is held constant (i.e., signal power equalization over all time channel realizations). Although the lower bound fails when the interference is held constant, we later show numerically that, since the distribution on the SINR is a function of both channel realizations and beamforming weights, the lower bound will hold for the channels of interest in this work. Therefore, (A.3) is a constrained lower bound.

Since the MMSE-CDIT beamforming algorithm maximizes a bound rather than the exact ergodic capacity, we are interested in the tightness of each bound. For small SINR $\sigma_s^2/\sigma_n^2 \ll 1$ the ergodic capacity can be approximated using a first-order Taylor series expansion on the natural logarithm

$$\begin{aligned} C &= E \left[\log \left(1 + \frac{\sigma_s^2 s}{\sigma_n^2 n} \right) \right] \\ &= \sum_{i=1}^{i=\infty} \frac{(-1)^i}{(2i)!} E \left[\left(\frac{\sigma_s^2 s}{\sigma_n^2 n} \right)^i \right], \quad \frac{\sigma_s^2 s}{\sigma_n^2 n} < 1 \quad (\text{A.4}) \\ &\approx E \left[\frac{\sigma_s^2 s}{\sigma_n^2 n} \right] \approx C^{\text{upper}}, \end{aligned}$$

where the final approximation comes from applying the same expansion to (A.2). For larger SINR $\sigma_s^2/\sigma_n^2 \gg 1$, the ergodic

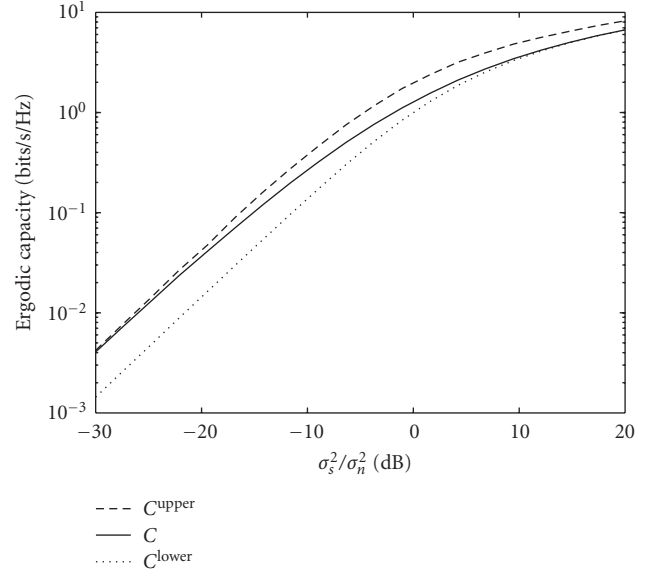


FIGURE 9: Ergodic capacity with upper and lower bounds in an interference limited, single-user system with $m = 3$ degrees of freedom.

capacity can be approximated by

$$\begin{aligned} C &\approx E \left[\log \left(\frac{\sigma_s^2 s}{\sigma_n^2 n} \right) \right] \\ &= E[\log(\sigma_s^2 s)] - E[\log(\sigma_n^2 n)] \\ &= \log(\sigma_s^2) - \log(\sigma_n^2) + E[\log(s)] - E[\log(n)] \quad (\text{A.5}) \\ &= \log \left(\frac{\sigma_s^2 E[s]}{\sigma_n^2 E[n]} \right) \approx C^{\text{lower}}, \end{aligned}$$

where $E[\log(s)] - E[\log(n)] = 0$ if we assume that s and n are i.i.d. random variables. Figure 9 plots ergodic capacity with upper and lower bounds as a function of SINR when s and n are chi-squared random variables each with three degrees of freedom and a base-2 logarithm. Figure 10 results are for measured data with various initial positions for $N_t = 4$, $N_r = 1$, $K = 6$, and $P = 10$. The optimal beamforming weights are found using the CO-RCI algorithm and then fixed as the channel changes over time. Similar results were demonstrated for a variety of different datasets over all possible starting displacements and various beamforming algorithms.

The results show that C^{upper} is tight for small SINR while C^{lower} is a better approximation for large SINR. Since this work focuses on the high-capacity, multiuser, broadcast channel, the high SINR region in Figure 9 is of interest, suggesting that the lower bound provides a tighter approximation to the actual ergodic (or sample) capacity and should be used for the MMSE-CDIT beamforming algorithm. It should be noted that (1) with beamforming the signal gains will not necessarily follow the same distribution as the interference plus noise and (2) the bound results from

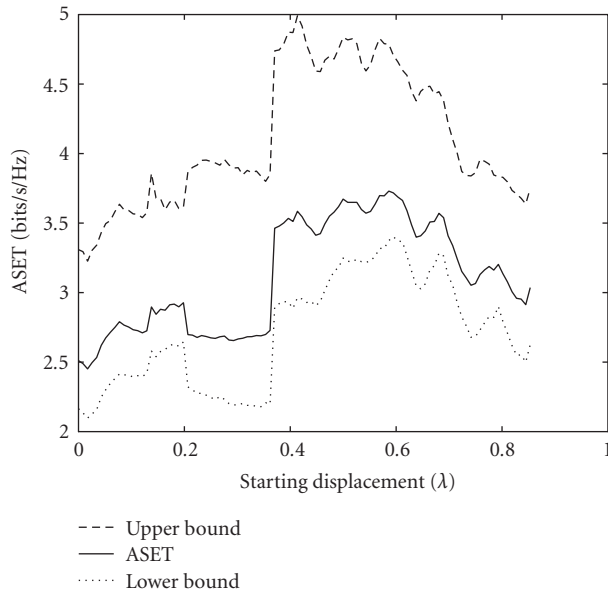


FIGURE 10: The average sample expected throughput (ASET) with upper and lower bounds for various initial displacements. The measured channel was used for a system with $N_t = 4$, $N_r = 1$, $K = 6$, and $P = 10$.

Figure 9 suggest performance in an ideal case. Even with these limitations, however, the results in Figure 10 on bound tightness still hold.

ACKNOWLEDGMENT

This work was sponsored by the U.S. Army Research Office under the Multi-University Research Initiative (MURI) Grant no. W911NF-04-1-0224.

REFERENCES

- [1] A. Goldsmith, S. A. Jafar, N. Jindal, and S. Vishwanath, "Capacity limits of MIMO channels," *IEEE Journal on Selected Areas in Communications*, vol. 21, no. 5, pp. 684–702, 2003.
- [2] J. W. Wallace, M. A. Jensen, A. Gummalla, and H. B. Lee, "Experimental characterization of the outdoor MIMO wireless channel temporal variation," *IEEE Transactions on Vehicular Technology*, vol. 56, no. 3, pp. 1041–1049, 2007.
- [3] J. W. Wallace and M. A. Jensen, "Time varying MIMO channels: measurement, analysis, and modeling," *IEEE Transactions on Antennas and Propagation*, vol. 54, no. 11, pp. 3265–3273, 2006.
- [4] T. Yoo and A. Goldsmith, "Capacity and power allocation for fading MIMO channels with channel estimation error," *IEEE Transactions on Information Theory*, vol. 52, no. 5, pp. 2203–2214, 2006.
- [5] S. Yang and J. Belfiore, "The impact of channel estimation error on the DPC region of the two-user Gaussian broadcast channel," in *Proceedings of the 43rd Annual Allerton Conference on Communication, Control, and Computing*, Monticello, Ill, USA, September 2005.
- [6] J. Jootar, J. R. Zeidler, and J. G. Proakis, "On the performance of concatenated convolutional code and alamouti space-time code with noisy channel estimates and finite depth interleaving," to appear in *IEEE Transactions on Communications*.
- [7] J. Jootar, J. R. Zeidler, and J. G. Proakis, "On the performance of closed-loop transmit diversity with noisy channel estimates," to appear in *IEEE Transactions on Communications*.
- [8] E. Visotsky and U. Madhow, "Space-time transmit precoding with imperfect feedback," *IEEE Transactions on Information Theory*, vol. 47, no. 6, pp. 2632–2639, 2001.
- [9] S. Jafar, S. Vishwanath, and A. Goldsmith, "Channel capacity and beamforming for multiple transmit and receive antennas with covariance feedback," in *Proceedings of the International Conference on Communications (ICC '01)*, vol. vol. 7, pp. 2266–2270, Helsinki, Finland, June 2001.
- [10] M. Sanchez-Fernandez and A. Lozano, "Doppler sensitivity of link reciprocity in TDD MIMO systems," in *Proceedings of IEEE Global Telecommunications Conference (GLOBECOM '05)*, vol. vol. 5, pp. 3073–3076, St. Louis, Mo, USA, November–December 2005.
- [11] A. Vakili, M. Sharif, and B. Hassibi, "The effect of channel estimation error on the throughput of broadcast channels," in *Proceedings of the 31st IEEE International Conference on Acoustics, Speech and Signal Processing (ICASSP '06)*, vol. vol. 4, pp. 29–32, Toulouse, France, May 2006.
- [12] A. Dana, M. Sharif, and B. Hassibi, "On the capacity region of multi-antenna Gaussian broadcast channels with estimation error," in *Proceedings of the IEEE International Symposium on Information Theory (ISIT '06)*, pp. 1851–1855, Seattle, Wash, USA, July 2006.
- [13] P. Viswanath and D. N. C. Tse, "Sum capacity of the vector Gaussian broadcast channel and uplink-downlink duality," *IEEE Transactions on Information Theory*, vol. 49, no. 8, pp. 1912–1921, 2003.
- [14] P. Ding, D. J. Love, and M. D. Zoltowski, "On the sum rate of multi-antenna broadcast channel with channel estimation error," in *Proceedings of the 39th Asilomar Conference Signals, Systems and Computers*, pp. 1524–1528, Pacific Grove, Calif, USA, October–November 2005.
- [15] Q. H. Spencer, J. W. Wallace, C. B. Peel, T. Svantesson, A. Lee Swindlehurst, and A. Gummalla, "Performance of multi-user spatial multiplexing with measured channel data," in *MIMO System Technology and Wireless Communications*, CRC Press, Boca Raton, Fla, USA, 2006.
- [16] R. Doostnejad, T. J. Lim, and E. Sousa, "Precoding for the MIMO broadcast channels with multiple antennas at each receiver," in *Proceedings of the 39th Annual Conference on Information Sciences and Systems (CISS '05)*, Baltimore, Md, USA, March 2005.
- [17] M. Schubert and H. Boche, "Iterative multiuser uplink and downlink beamforming under SINR constraints," *IEEE Transactions on Signal Processing*, vol. 53, no. 7, pp. 2324–2334, 2005.
- [18] M. Stojnic, H. Vikalo, and B. Hassibi, "Rate maximization in multi-antenna broadcast channels with linear preprocessing," in *Proceedings of IEEE Global Telecommunications Conference (GLOBECOM '04)*, vol. vol. 6, pp. 3957–3961, Dallas, Tex, USA, November–December 2004.
- [19] W. Jakes, *Microwave Mobile Communications*, John Wiley & Sons, New York, NY, USA, 1974.
- [20] D.-S. Shiu, G. J. Foschini, M. J. Gans, and J. M. Kahn, "Fading correlation and its effect on the capacity of multielement

- antenna systems," *IEEE Transactions on Communications*, vol. 48, no. 3, pp. 502–513, 2000.
- [21] T. Fugen, C. Kuhnert, and W. Wiesbeck, "Capacity of the MIMO broadcast channel under realistic propagation conditions," in *Proceedings of the 16th International Symposium on Personal, Indoor and Mobile Radio Communications (PIMRC '05)*, vol. vol. 4, pp. 2660–2664, Berlin, Germany, September 2005.
- [22] M. Herdin, N. Czink, H. Özcelik, and E. Bonek, "Correlation matrix distance, a meaningful measure for evaluation of non-stationary MIMO channels," in *Proceedings of the 61st IEEE Vehicular Technology Conference (VTC '05)*, vol. vol. 1, pp. 136–140, Stockholm, Sweden, May-June 2005.
- [23] J. W. Wallace, M. A. Jensen, A. L. Swindlehurst, and B. D. Jeffs, "Experimental characterization of the MIMO wireless channel: data acquisition and analysis," *IEEE Transactions on Wireless Communications*, vol. 2, no. 2, pp. 335–343, 2003.
- [24] K. Yu, M. Bengtsson, B. Ottersten, D. McNamara, P. Karlsson, and M. Beach, "Second order statistics of NLOS indoor MIMO channels based on 5.2GHz measurements," in *Proceedings of Conference IEEE Global Telecommunications Conference (GLOBECOM '01)*, vol. vol. 1, pp. 156–160, San Antonio, Tex, USA, November 2001.
- [25] H. Özcelik, M. Herdin, W. Weichselberger, J. W. Wallace, and E. Bonek, "Deficiencies of 'Kronecker' MIMO radio channel model," *Electronics Letters*, vol. 39, no. 16, pp. 1209–1210, 2003.
- [26] B. T. Maharaj, J. W. Wallace, and M. A. Jensen, "A low-cost open-hardware wideband multiple-input multiple-output (MIMO) wireless channel sounder," to appear in *IEEE Transactions on Instrumentation and Measurement*.
- [27] V. R. Anreddy and M. A. Ingram, "Capacity of measured Ricean and Rayleigh indoor MIMO channels at 2.4GHz with polarization and spatial diversity," in *Proceedings of IEEE Wireless Communications and Networking Conference (WCNC '06)*, vol. vol. 2, pp. 946–951, Las Vegas, Nev, USA, April 2006.
- [28] J. Chung, C.-S. Hwang, K. Kim, and Y. K. Kim, "A random beamforming technique in MIMO systems exploiting multiuser diversity," *IEEE Journal on Selected Areas in Communications*, vol. 21, no. 5, pp. 848–855, 2003.
- [29] S. Boyd and L. Vandenberghe, *Convex Optimization*, Cambridge University Press, Cambridge, UK, 2004.

Special Issue on Dependable Semantic Inference

Call for Papers

After many years of exciting research, the field of multimedia information retrieval (MIR) has become mature enough to enter a new development phase—the phase in which MIR technology is made ready to get adopted in practical solutions and realistic application scenarios. High users' expectations in such scenarios require high dependability of MIR systems. For example, in view of the paradigm “getting the content I like, anytime and anyplace” the service of consumer-oriented MIR solutions (e.g., a PVR, mobile video, music retrieval, web search) will need to be at least as dependable as turning a TV set on and off. Dependability plays even a more critical role in automated surveillance solutions relying on MIR technology to analyze recorded scenes and events and alert the authorities when necessary.

This special issue addresses the dependability of those critical parts of MIR systems dealing with semantic inference. Semantic inference stands for the theories and algorithms designed to relate multimedia data to semantic-level descriptors to allow content-based search, retrieval, and management of data. An increase in semantic inference dependability could be achieved in several ways. For instance, better understanding of the processes underlying semantic concept detection could help forecast, prevent, or correct possible semantic inference errors. Furthermore, the theory of using redundancy for building reliable structures from less reliable components could be applied to integrate “isolated” semantic inference algorithms into a network characterized by distributed and collaborative intelligence (e.g., a social/P2P network) and let them benefit from the processes taking place in such a network (e.g., tagging, collaborative filtering).

The goal of this special issue is to gather high-quality and original contributions that reach beyond conventional ideas and approaches and make substantial steps towards dependable, practically deployable semantic inference theories and algorithms.

Topics of interest include (but are not limited to):

- Theory and algorithms of robust, generic, and scalable semantic inference
- Self-learning and interactive learning for online adaptable semantic inference

- Exploration of applicability scope and theoretical performance limits of semantic inference algorithms
- Modeling of system confidence in its semantic inference performance
- Evaluation of semantic inference dependability using standard dependability criteria
- Matching user/context requirements to dependability criteria (e.g., mobile user, user at home, etc.)
- Modeling synergies between different semantic inference mechanisms (e.g., content analysis, indexing through user interaction, collaborative filtering)
- Synergetic integration of content analysis, user actions (e.g., tagging, interaction with content) and user/device collaboration (e.g., in social/P2P networks)

Authors should follow the EURASIP Journal on Image and Video Processing manuscript format described at <http://www.hindawi.com/journals/ivp/>. Prospective authors should submit an electronic copy of their complete manuscripts through the journal Manuscript Tracking System at <http://mts.hindawi.com/>, according to the following timetable:

| | |
|------------------------|------------------|
| Manuscript Due | November 1, 2008 |
| First Round of Reviews | February 1, 2009 |
| Publication Date | May 1, 2009 |

Guest Editors

Alan Hanjalic, Delft University of Technology, 2600 AA Delft, The Netherlands; a.hanjalic@tudelft.nl

Tat-Seng Chua, National University of Singapore, Singapore 119077; chuats@comp.nus.edu.sg

Edward Chang, Google Inc., China; University of California, Santa Barbara, CA 93106, USA; echang@ece.ucsb.edu

Ramesh Jain, University of California, Irvine, CA 92697, USA; jain@ics.uci.edu